EFECTS OF THE ENVIRONMENT ON STABLE CRACK GROWTH IN HIGH-STRENGTH STEELS UNDER STATIC AND CYCLIC LOADING

L. Hyspecká [+/], M. Tvrdý [+/], K. Mazanec [++/]

[+/] Research Institute of Vítkovice Steel and Engineering Works, 706 02 Ostrava, Czechoslovakia

[++/] Technical University, 708 33 Ostrava, Czechoslovakia

ABSTRACT

The paper describes a study of the way a corrosive environment restricts the technical applicability of an ultra-high strength steel of the 30 MnSiMo type, with a structure of low-tempered martensite and a tensile strength in the 1490 to 1820 MPa range. The work examined the effects of the metallurgical and structural characteristics on the fracture toughness, on the K_{ISCC} value, and on the kinetics of fatigue crack propagation in a corrosive environment, in air, and in a vacuum. The data recorded on a set of melts were processed statistically to establish the dependences of the above parameters on the tensile strength, and, in the corrosion fatigue investigations, also to ascertain the influence of the cycle frequency in dependence on the ΔK value. This work helped to define the guidelines and constraints governing the practical utilization of this steel.

KEYWORDS

Stress corrosion cracking; hydrogen embrittlement; corrosion fatigue; influence of frequences.

INTRODUCTION

Corrosive environments can severely limit the technical applicability of ultra-high strength steels with microstructures of low-tempered martensite, which attain tensile strengths over 1500 MPa. These limitations become apparent both under static and under cyclic loading conditions. Although conventional investigations of the mechanical properties or fracture toughness of such steels fail to reveal any substantial microstructural and metallurgy effects, those effects become clearly evident when the testing is conducted in aggressive media, as will be shown in the present paper.

EXPERIMENTAL MATERIALS AND TECHNIQUES

This research was performed on a set of routine melts of 30 MnSiMo [30 Mn1.5Si1.0Mo0.30] steel, where the carbon contents ranged from 0.26 to 0.34 per cent. The specimens were taken from plates 14 mm thick, after their heat treatment by water quenching from 910°C and subsequent tempering for 2 hours at 230°C. This treatment left the plates with a structure of low-tempered martensite. The mechanical properties and brittle fracture characteristics were established on specimens taken in the rolling LT direction. The fracture toughness testing was performed by the standard technique on single-edge notch [SEN] specimens 12 mm thick in three-point bending. The stress corrosion cracking tests for ascertaining the threshold value of K_{ISCC} were carried out on tensile SEN specimens 10 mm thick, in a 3.5 % aqueous solution of NaCl /Tvrdý, Hyspecká, Mazanec, 1978/. The stable crack growth rate was investigated by means of a compliance technique described previously /Tvrdý and others, 1977/.

The tests under cyclic loading conditions were conducted on 3 mm thick specimens provided with a central notch. These specimens were subjected to sinusoidal loading cycles, at a constant load amplitude and at R = 0, on a servohydraulic testing machine at frequencies of 0.45, 2 and 6 Hz in distilled water or in air, and at 6 Hz in a vacuum of the order 10^{0} Pa. This work determined the dependence of the fatique crack growth rate per cycle, d21/dN, upon the stress intensity range ΔK. Next, a scanning electron microscope was employed to establish the average proportion of intercrystalline failure on the fracture surfaces for each of the ΔK values; this was done by the abscissa method, in sets of ten adjacent squares with sides measuring 130 microns each, at a magnification of 1000 X.

The surface segregation of various elements was examined by the AES method, on specimens 8 mm in diameter and 2 mm thick. The specimens were cleaned before their insertion in the apparatus, and then subjected to ionic etching, within the apparatus, to remove a surface layer about one micron thick, preliminary to the Auger electron spectroscopy which established their basic spectrum. The specimens were then annealed, by 10 minutes at each temperature rising from 400 to 1100°C; after every heating period and measurement, a layer about 0.1 micron thick was removed from the surface by ionic etching. The spectra thus obtained were evaluated by means of linear interpolation /Tvrdý, Hyspecká, Mazanec, 1979/.

RESULTS AND DISCUSSION

Fig. 1 presents a set of K_{IC} fracture toughness data obtained in testing at +20 and -40°C. The diagram shows that, in this type of steel and within the examined range of tensile strengths R_m , no statistically significant relationship was detected between the K_{IC} and R_m values. All the values plotted in this diagram are the averages of three or more measurements on each of the investigated melts. The data in this diagram display a considerable degree of scatter,although the figures for the individual melts did not exceed the scatter only 10 per cent each way, which Knott /1975/ claims to be the limit of reproducibility in K_{IC} measurements. This implies that the mean K_{IC} figures ascertained on the various melts are likely to have been

influenced by metallurgical factors. That observation led to a statistical analysis of the recorded K_{IC} values, based on the assumption that they would conform to a Weibull-type distribution. The statistical lower bound value for K_{IC} data obtained at -40°C, was 60 MPa.$m^{1/2}$. Fractographic analyses proved that the fracture surfaces formed at both of the testing temperatures were of transcrystalline ductile character.

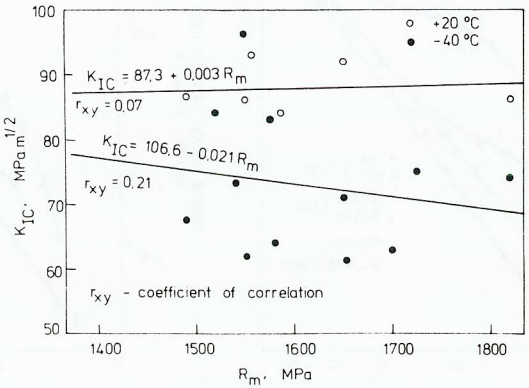

Fig. 1. Dependence of the fracture toughness K_{IC} on the tensile strength.

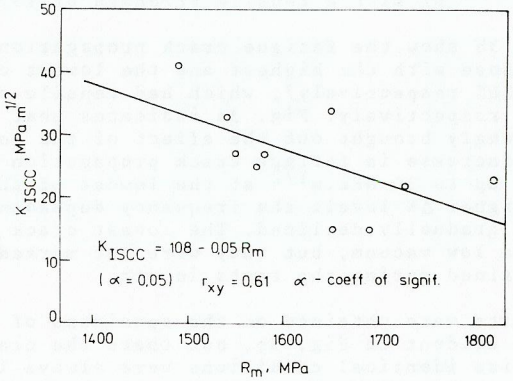

Fig. 2 Dependence of the K_{ISCC} value on the tensile strength.

Fig. 2 is a plot of the threshold values of K_{ISCC} in dependence on the R_m level; it demonstrates that, even in the narrow interval of R_m values examined in this work, K_{ISCC} tends to diminish as the tensile strength increases. A significant finding, confirmed on all the specimens, was that the dependence of the stable crack propagation rate on the instantaneous stress intensity factor K_I always displayed a stationary region [marked II] in the 45 to 60 MPa.$m^{1/2}$ interval; this corresponded to a crack growth rate of 1.7 . 10^{-5} to 12.0.10^{-5}

mm.s^{-1}. Microfractographic investigations revealed that the failures were predominantly intercrystalline [roughly 80 per cent], and that they had taken place along the prior austenite grain boundaries.

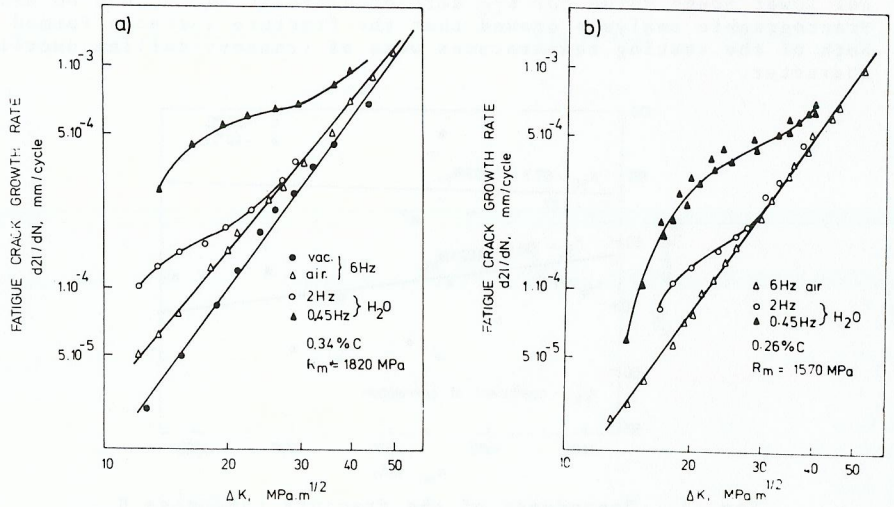

Fig. 3 Kinetics of fatigue crack growth in a steel
a/ with a tensile strength of 1820 MPa,
b/ with a tensile strength of 1570 MPa.

Figs. 3a and 3b show the fatigue crack propagation rates for two selected melts, those with the highest and the lowest carbon contents [0.34 and 0.26% respectively], which had tensile strengths R_m of 1820 and 1570 MPa respectively. Fig. 3a indicates that an aqueous environment had strongly brought out the effect of the loading frequency. The highest increase in fatigue crack propagation rates were recorded at ΔK values up to 30 MPa.m$^{1/2}$ at the lowest of the frequencies, 0.45 Hz, but at higher ΔK levels the frequency dependence of the crack growth rates gradually declined. The lowest crack growth rates were detected in a low vacuum, but they were not markedly lower than the rates ascertained during the tests in air.

Similar results were obtained on the specimens of the lower-strength steel, as is evident in Fig. 3b, but there the crack propagation rates under otherwise identical conditions were always lower than in the higher-strength material. For instance, a steel with an R_m of 1820 MPa, tested in water at a ΔK of 20 MPa.m$^{1/2}$, displayed a crack growth rate of 5.4 . 10^{-4} mm per cycle at 0.45 Hz, but this declined to 1.85 . . 10^{-4} mm/cycle at 2 Hz. When these tests, again in water at a ΔK of 20 MPa.m$^{1/2}$, were repeated on a steel with an R_m of only 1570 MPa, the crack growth rate dropped to 2.99 . 10^{-4} mm/cycle at 0.45 Hz, and to a mere 1.32 . 10^{-4} mm/cycle at 2 Hz.

For the dependence illustrated in Fig. 3a, the chart in Fig. 4a shows the percentual proportions of intercrystalline fracture ascertained in the melt with the highest tensile strength. All the specimens exhibited also striation zones on their fracture surfaces, but always to a limited extent only. The specimens that had been tested in water

bore signs of slight corrosion, but these were nowhere pronounced enough to preclude a quantitative fractographic investigation of those specimens.

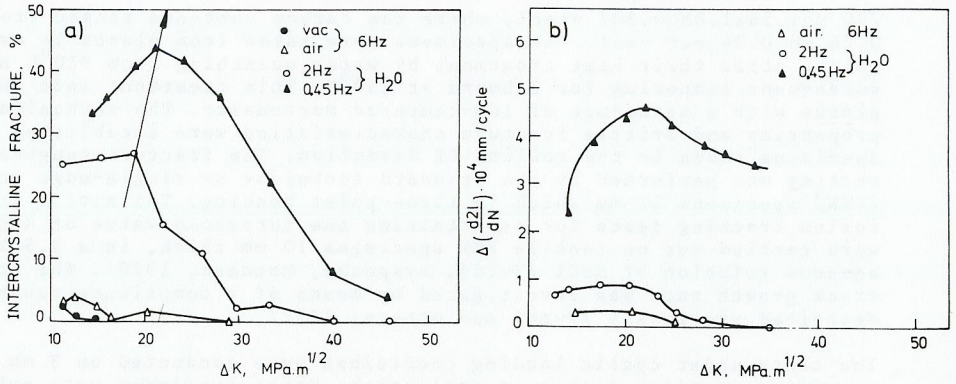

Fig. 4 Dependence of both the proportion of intercrystalline fracture /a/ and the difference between the fatigue crack propagation rates in a corrosive environment and in vacuum /b/ on ΔK.

Fig. 4b summarizes the differences between the fatigue crack propagation rates in the examined media at the examined frequencies, and the rates observed in a vacuum. When the tests were conducted in water, the maxima of the curves in both Figs. 4a and 4b shifted towards higher ΔK values as the loading frequency declined, as is marked by the arrows on the diagrams. It will be noted that the maxima of the proportion of intercrystalline fracture roughly coincide with the maximum differences between the crack propagation rates. An approximate extrapolation of the maxima to the level of an 80 per cent proportion of intercrystalline failure [which is the proportion detected at a K_I value close above the K_{ISCC} level] indicates that at very low loading frequencies, i.e. in conditions approaching a static mode of loading the maximum in Fig. 4a would be displaced to a ΔK value around 25 MPa.m$^{1/2}$. Reference to Fig. 2 shows that this value practically corresponds to the K_{ISCC} level ascertained in this melt.

We may infer from these results that at low loading frequencies, the outcome will largely be decided by the processes which govern the propagation of cracks in stress corrosion cracking. Let us now examine the implications of the assumption that this crack growth is governed primarily by the transfer of hydrogen-either by the mechanism proposed by Frandsen and Marcus /1975/, i.e. by mobile dislocations dragging the hydrogen atoms into the plastic zone of the advancing crack, or else in a model founded on the conditions existing for the volume diffusion of hydrogen. First mechanism appears to be ruled out by the fact that, in view of the intercrystalline nature of the fractures, at a ΔK of 21 MPa.m$^{1/2}$ the plastic zone dimensions were only R_{pf} = = 15.2 microns, or r_{pf} = 3.8 microns, and thus much smaller than the average size of the prior austenitic grains, which was 20 microns. The alternative explanation needs rests on the assumption that the hydrogen concentration will vary both with ΔK and with the load

cycling frequency, because the postulated higher hydrogen concentration in the plastic zone can arise only if enough time is available for the volume diffusion of hydrogen; that would correspond to the ascending parts of the curves in Figs. 4a and 4b. At ΔK levels higher than the maxima in Figs. 4a and 4b, however, the fatigue crack propagation rate will clearly be so high as to keep the hydrogen concentration in the plastic zone at the crack tip fairly low, simply because there will be too little time for this concentration to build up appreciably.

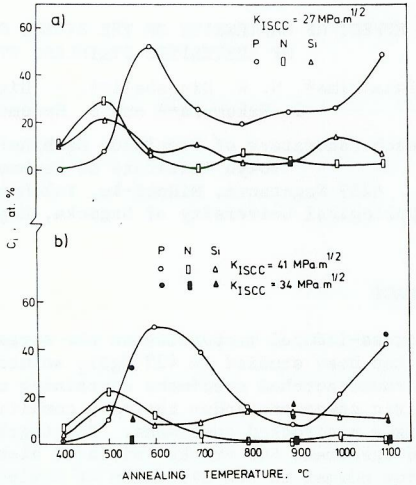

Fig. 5 Surface concentrations of impurity elements at various annealing temperatures
a/ in a steel with a K_{ISCC} of 27 MPa.m$^{1/2}$
b/ in steels with K_{ISCC} values of 41 and 34 MPa.m$^{1/2}$.

Apart from hydrogen, the intergranular nature of brittle failures can also be influenced by microsegregation of impurity elements, especially by phosphorus and nitrogen /Briant, Banerji, 1978/. Figs. 5a and 5b show how the surface segregations of those two elements, and of silicon, varied with the annealing temperature in three melts which had different K_{ISCC} values. Fig. 5a applies to a melt with a K_{ISCC} level of 27 MPa. m$^{1/2}$, Fig. 5b to melts with 41 and 34 MPa.m$^{1/2}$ respectively. The material covered by Fig. 5a was inferior to the other two melts in the cohesion of its grain boundaries under conditions conducive to stress corrosion cracking; and the diagram confirms that in this material, austenitizing at 900°C had produced a significantly higher surface concentration of phosphorus, as well as a slight rise in the nitrogen concentration. Both of these elements have been reported as contributing to intercrystalline failures along the prior austenitic grain boundaries in low-tempered martensite /Banerji, McMahon, Feng, 1978/. Fig. 5b indicates that the surface concentrations of silicon at 900°C were greater in the two melts with the higher K_{ISCC} values. One possible explanation for this finding would be that silicon, segregating at the grain boundaries, does not cause as pronounced embrittlement as phosphorus and nitrogen do. An alternative interpretation would be that in the melt covered by Fig. 5a, the embrittling effect of silicon was obscured by the far more profound

effects of the phosphorus and nitrogen concentrations.

The results point to the conclusion that, in these economically alloyed steels of the 30 MnSiMo type, the conventional mechanical property investigations are not sufficient in themselves. Any assessment of those properties must always take into account the various modifying effects, such as the metallurgical characteristics of the melt in question or the environmental effects on the material under the envisaged service conditions.

The evaluation procedure outlined above has permitted a more precise and dependable definition of the conditions that limit the technical applicability of this steel, because it revealed the lower bound envelope of fracture toughness values under both static and cyclic loading, as well as the way these bounds are affected by the concurrent effects of corrosive environments.

CONCLUSIONS

i/ In economically alloyed ultra-high strength steels of the 30MnSiMo [30Mn1.5Si1.0Mo0.30] type, with a structure of low-tempered martensite and tensile strength of 1490 to 1820 MPa, no evidence was found that the K_{IC} level in any way depends on the tensile strength. The statistical lower bound value of fracture toughness at -40°C was 60 MPa.m$^{1/2}$.

ii/ Statistical processing of the K_{ISCC} values recorded in an aqueous solution of NaCl confirmed that they are strength dependent, even within the narrow interval of tensile strengths examined in this work. A plot of the crack growth rates versus the instantaneous K_I values displayed a stationary region, where the growth rate varied between 1.7 and 12.0 . 10^{-5} mm.s^{-1}, and which occurred in the 45 to 60 MPa.m$^{1/2}$ range; in these cases the cracks propagated predominantly, by about 80 per cent, by an intercrystalline mechanism.

iii/ Pronounced environmental effects were also detected under cyclic loading conditions. Both the fatigue crack growth rate and the percentage of intercrystalline fracture, at comparable magnitudes of ΔK, were found to grow as the cycle frequency diminished. An extrapolation of the recorded maxima of intercrystalline fracture yielded close agreement between the ΔK value corresponding to an 80 per cent proportion of intercrystalline failure and the K_{ISCC} level established in this study.

iv/ The predominantly intercrystalline nature of the fractures ascertained in this work may also be partly attributable to the microsegregation of impurity elements [phosphorus and nitrogen] at the prior austenite grain boundaries.

REFERENCES

Banerji, S. K., C. J. McMahon, Jr., and H. C. Feng /1978/. Intergranular fracture in 4340 type steels: effect of impurities and hydrogen. Met. Trans., 9A, 237-247.

Briant, C. L., and S. K. Banerji /1978/. Intergranular failure in steel: the role of grain boundary composition. Int. Metall. Rev., 23, 164-199.

Frandsen, J. D., and H. L. Marcus /1975/. The correlation between grain size and plastic zone size for environmental hydrogen assisted fatigue crack propagation. Scripta Met., 9, 1089-1094.

Knott, J. F. /1975/. Critical assessment of fracture mechanics. Met. Sci., 9, 445-447.

Tvrdý, M., V. Suchánek, L. Hyspecká, and K. Mazanec /1977/. Effect of metallurgy on stress corrosion cracking and hydrogen embrittlement of ultrahigh strength steels. In D. M. R. Taplin /Ed./, Fracture 1977 - ICF4, Vol. 2. University of Waterloo Press, Waterloo. pp. 255-259.

Tvrdý, M., L. Hyspecká, and K. Mazanec /1978/. Effect of high temperature thermomechanical treatment on mechanical metallurgy characteristics of high strength martensitic steels. Met. Technol., 5, 73-78.

Tvrdý, M., L. Hyspecká, and K. Mazanec /1979/. Evaluation of fracture toughness of HAZ after stress relief treatment. In Practical Applications of Fracture Mechanics to the Prevention of Failure of Welded Structures, IIW Annual Assembly, IIW, Bratislava. pp. 175-182.